Journal of Materials and Environmental Sciences
ISSN : 2028-2508
CODEN : JMESCN

J. Mater. Environ. Sci., 2020, Volume 11, Issue 4, Page 933-946

http://www.jmaterenvironsci.com

Organic compounds based on pyrrole and terphenyl for organic light-emitting diodes (OLED) applications: Design and electro-optical properties

M. Raftani[1], T. Abram[3], R. Kacimi[3], M. N. Bennani[2] and M. Bouachrine[1, 3*]

[1]*Molecular Chemistry and Natural Substances Laboratory, Faculty of Science, Moulay Ismail University Meknes, Morocco*
[2]*Laboratory of Chemistry and Biology Applied to the Environment, Faculty of Science, My Ismail University Meknes, Morocco*
[3]*MEM (LASMAR) ESTM, University Moulay Ismail, Meknes, Morocco*

Received 19 Nov 2019,
Revised 18 Mar 2020,
Accepted 19 Mar 2020

Keywords
- ✓ *OLED,*
- ✓ Terphenyl ,
- ✓ Pyrrole,
- ✓ DFT,
- ✓ B3LYP.

bouachrine@gmail.com

Abstract

In order to propose new organic materials for organic light emitting diodes (OLEDs) applications, we present in this work a computational study based on quantum chemistry on molecular materials based on terphenyl and pyrrole. We report the study of the structural and electronic properties of three molecules C_1 (pyrrole-terphenyl-terphenyl-pyrrole), C_2 (pyrrole-terphenyl-pyrrole-terphenyl) and C_3 (terphenyl-pyrrole-pyrrole-terphenyl). The geometry of these studied compounds was obtained after optimization in their fundamental states by using the functional density theory (DFT) with the B3LYP method and the basis set 6-311G (d, p). The studied electronic properties determined from the most stable conformation of each studied molecule are the HOMO, LUMO, the gap energies, electron affinity (EA), ionization potential (IP) and NBO analysis. The time-dependent density theory method TD-DFT-B3LYP 6-311G (d, p)was used for the study of absorption and emission properties. Based on these different optoelectronic, absorption and emission properties, we will discuss the effect of the regularity of the sequence on the studied properties and then propose new structures to experimenters for synthesis and OLED applications.

1. Introduction

Currently, materials based on π-conjugated organic molecules constitute an important class of materials with remarkable properties leading to a huge field of research in both chemistry and physics [1]. These materials are considered good candidates for optoelectronic applications and especially research on new low cost organic photovoltaic devices [2]. This is due to their specific properties such as photochemical and thermal stability and also the high load mobility [3]. Recall that π-conjugated molecules are already widely used in many organic optoelectronic devices, including organic light-emitting diodes (OLEDs) [4], organic field-effect transistors (OFETs) [5], organic resonant tunnel diodes [6, 7], organic phototransistors [8], organic photovoltaic cells [9] and organic photo detectors [10]. Electroluminescent devices based on these π-conjugated organic systems are of great interest because of their important physicochemical characteristics and are considered the devices of tomorrow.

The first organic light-emitting diode (OLED) devices were invented by Tang and VanSlyke in 1987 [11, 12]. After this discovery, many research works appeared and the results are encouraging. In 1998, a team of researchers from Princeton University and the University of Southern California were the first to produce highly efficient OLEDs based on the light emitting mechanism, called electrophoresis OLED or

simply phosphorescent (OLED) [13]. An OLED is defined as a device that emits light under the application of an external voltage. The organic electroluminescence is summarized as follows: after an application of a voltage V on an organic semiconductor, the holes in the valence band (BV) and the electrons in the conduction band (BC) are injected. Electron-hole recombination causes light emission [14, 15]. The color of the emitted light depends on the difference in energy level between the BV and the BC and the Coulomb force tying the electron to the hole during recombination [16]. Currently, OLEDs have been remarkably successful, attracting considerable industry. There are two main applications of OLED devices: OLED displays and OLED lighting. Samsung, Sony and LG are among the most important companies selling OLED screens for TVs and mobile phones. OLED displays have advantages over LCDs, such as thinner size, lower power consumption, higher contrast ratio, shorter response time, higher brightness, and flexibility. For OLED lighting, OLEDs do not dazzle heat, are economical and have a long life.

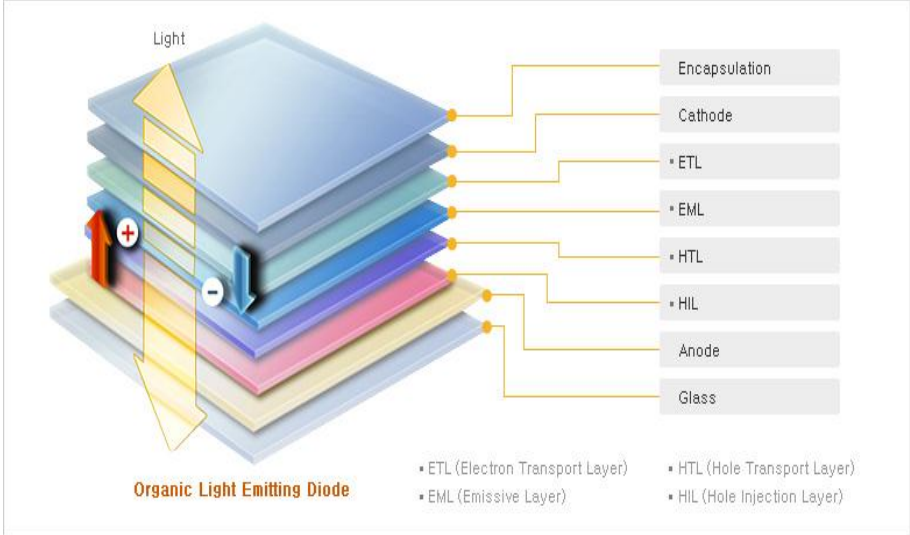

Figure 1: *The compositions of OLED, compose of cathode electrode, electron transport layer (ETL),hole blocking layer (HBL), emissive layer (EL), hole transport layer (HTL), hole injection layer (HIL),anode electrode , glass substrate and encapsulation (protects from minor physical impacts).*

The OLED component in its simplest form consists of a single layer of organic material between the cathode and the anode, which is generally transparent and often consists of indium tin oxide (ITO). Organic thin films typically include a hole transport layer (HTL), an emission layer (EML) and an electron transport layer (ETL). By applying appropriate electrical voltage, the electrons and holes are injected into the EML layer from the cathode and the anode. The interaction of electron and hole pair at excited state is called exciton where its relaxation to the ground state can drive light emission. The charge transfer materials, the emitting layer, and the choice of electrodes are fundamental parameters that determine the performance and efficiency of an OLED component. In order to improve the efficiency of organic light-emitting materials [17-19], several works have recently been done, especially the study of short-chain luminescent compounds that can be used in an OLED structure [20]. This study often goes through a molecular design using the concepts of quantum chemistry in order to propose the desired electronic properties for this type of application before the synthesis, structures possessing.

In this context, we present in this work a computational study based on quantum chemistry on molecular materials based on terphenyl and pyrrole. We report the study of the structural and electronic properties of three molecules C_1 (pyrrole-terphenyl-terphenyl-pyrrole), C_2 (pyrrole-terphenyl-pyrrole-terphenyl) and C_3 (terphenyl-pyrrole-pyrrole-terphenyl) (Figure 2). The geometry of these studied compounds was

obtained after optimization in their fundamental states by using the functional density theory (DFT) with the B3LYP method and the basic set 6-311G (d, p) [21]. The studied electronic properties determined from the most stable conformation of each studied molecule are the HOMO, LUMO, the gap energies, electron affinity (EA), ionization potential (IP) and NBO analysis. The TD-DFT-B3LYP/6-311G (d, p) time-dependent density theory method was used for the study of absorption and emission properties. Based on these different optoelectronicproperties, we will propose in figure 2the structures to experimenters for synthesis and possibly for OLED applications.

2. Material and Methods

Currently, computations in quantum chemistry present a better tool for studying π-conjugated systems. The functional theory ofDFT density with the three-parameter Becke and Lee-Yang-Parr hybrid exchange functional method noted B3LYP [22-24] and the basis set 6-311G (d, p) was used for all studies. It is noted that these calculations are made with the Gaussian package 09 [24]. The geometric structures of molecules C_1, C_2 and C_3 at neutral cationic and anionic states have been optimized, and supported by a frequency calculation ensure that it is the absolute minimum. The energies of the HOMO, LUMO, bandgap and natural orbital bond (NBO) properties of these compounds were also determined from the optimized structures. In order to obtain detailed information on absorption and emission properties, such as absorption and electron emission wavelengths (λ_{max}), the corresponding oscillator forces and the excitation vertical energy, the TD-DFT-B3LYP / 6-311G method (d, p) was used.

3. Results and discussion

3.1. Geometries in the ground state

The geometrical parameters (distances and binding angles), of the three studied compounds in the ground-state are optimized by using the method B3LYP / 6-311G (d, p).To ensure that the optimized geometry of the compounds corresponds to the lowest point of the potential energy surface, frequency calculations are performed. The geometries of the optimized structures are presented in figure 2 and their geometrical parameters (the dielectric bond lengths di and dihedral angles θ_i) are listed in Table 1.

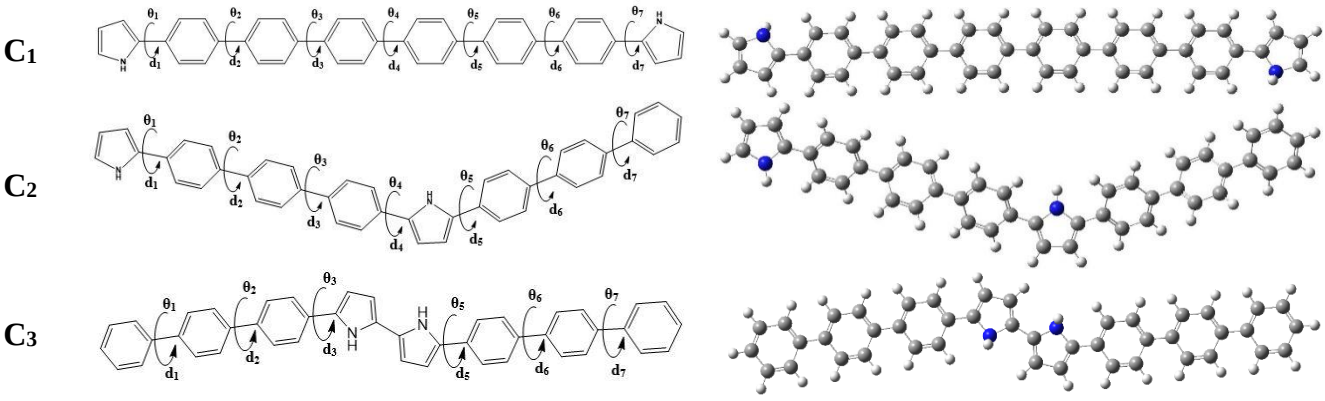

Figure 2: *Chemical structures and optimized ones of the studied compounds obtained by DFT / B3LYP / 6-311G (d, p).*

Table 1: *Values of the d_i (Å) binding lengths of the studied compounds obtained by B3LYP/ 6-311G (d, p).*

Molecules	d_1(Å)	d_2(Å)	d_3(Å)	d_4(Å)	d_5(Å)	D_6(Å)	D_7(Å)
C_1	1.46	1.48	1.48	1.48	1.48	1.48	1.46
C_2	1.48	1.48	1.46	1.46	1.48	1.48	1.46
C_3	1.48	1.48	1.46	1.44	1.46	1.48	1.48

Table 2: *Dihedral angle values (θ_i) of the studied compounds obtained by B3LYP / 6-311G (d, p).*

Molecules	θ_1	θ_2	θ_3	θ_4	θ_5	θ_6	θ_7
C_1	156.03	142.98	141.94	142.39	142.39	141.94	156.03
C_2	140.56	142.81	156.79	157.32	142.59	142.58	156.61
C_3	141.12	143.52	155.77	158.35	155.77	143.53	141.42

To have an efficient charge transport along the molecular chain, the studied molecules must have a good conjugation and a strong intermolecular interaction in order to facilitate the delocalization of the electrons [3]. The comparison of the geometrical parameters could provide predictive information on the said properties. To this end, we have determined from the optimized structures the inter-cyclic distances di and the intercyclic angles θi. We have noticed that the inter-cyclic distances di do not undergo significant variation as indicated in Table 1, the bond length values (di) vary from 1.44 Å to 1.48 Å, they decrease as they approach the pyrrole unit in all the molecules. These values tend towards double bonds which will facilitate internal charge transfer (ICT) between the cycles constituting each molecule and are comparable to those obtained by other authors on similar structures containing thiophene and phenylene [25, 26]. For the dihedral angles, the optimized geometries of these studied oligomers show that inter-cyclic torsion angles have values between 140 ° and 158° indicating that these three compounds have relatively twisted configurations.

3.2. Optoelectronic properties

To study optoelectronic properties, it is important to determine the energy levels of the highest occupied molecular orbital (HOMO) and the lowest unoccupied molecular orbital (LUMO) [27]. It is noted that these HOMO and LUMO energy levels play a key role in determining whether effective charge transfer will take place between the donor and the acceptor in electronic devices [25]. These parameters (HOMO and LUMO) can be calculated from the optimized structures obtained by the method B3LYP / 6311G (d, p) [28]. We have therefore determined for the three studied compounds C_1, C_2 and C_3 the energy of the HOMO level (E_{HOMO}), the LUMO level (E_{LUMO}) and the energy of the bandgap $E_{gap} = E_{LUMO} - E_{HOMO}$. These values are presented in Table 3.

Table 3: *Energy values of the electronic properties of the compounds studied.*

Molecules	E_{HOMO} (eV)	E_{LUMO} (eV)	E_{gap} (eV)
C_1	-5.356	-1.657	3.699
C_2	-5.156	-1.671	3.485
C_3	-4.866	-1.587	3.279

In π-conjugated systems, any increase in the length of the conjugation is accompanied by a destabilization of the HOMO energies and a stabilization of the LUMO energies [29]. According to Table 3, the values of the HOMO / LUMO energies are respectively: -5.356 / -1.657 eV for C_1, -5.156 / -1.671 eV for C_2 and -4.866 / -1.587 eV for C_3. The values of E_{gap} are 3.699 eV, 3.485 eV and 3.279 eV for C_1, $C_2$and C_3 respectively. We note that this energy "E_{gap}" decreases in the order $C_1 > C_2 > C_3$ indicating that when the two pyrrole units approach each other, the conjugation becomes better and consequentlythe gap energy decreases, this is probably due to the presence of the nitrogen atom in pyrrole which boosts the conjugation [28]. On the other hand, the examination of the highly occupied HOMO orbitals and the lowest virtual LUMO orbitals for the studied compounds is important because they can provide clear information on intramolecular load transfer (ICT) in such a system π-conjugated and the ability to transport electrons or holes [30]. Therefore, the electronic density isocontour of HOMO and LUMO of the studied compounds obtained by B3LYP/ 6-311G (d, p) is shown infigure 3. From this figure, it is noted that the electron

density of the HOMO and LUMO orbitals is distributed over the whole π-conjugate skeleton with a similar character. In general, HOMO's of all compounds have an anti-binder character between consecutive subunits and are located on the donor unit and π-separator, while LUMO has a binder character between sub-units and are centralized on the acceptor[31].

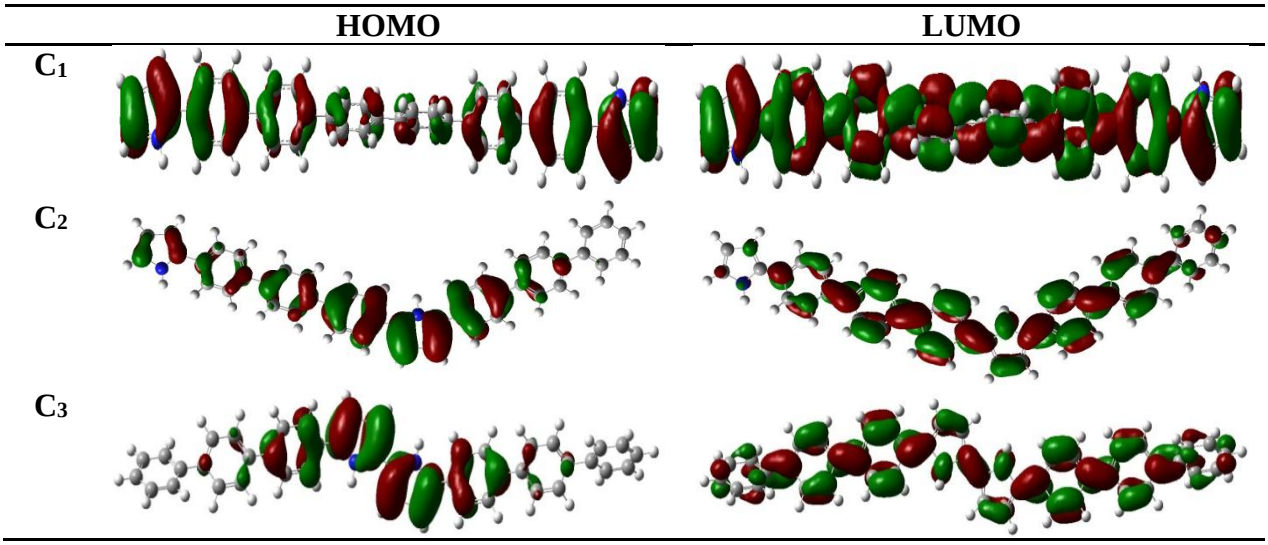

Figure 3: *The Electron density isocontours of the HOMO and LUMO orbitals of the compounds studied.*

In an electroluminescent device, the migration of holes from the injection layer (HIL) to the transport layer (HTL) / (EML) often depends on the energy levels of the HOMO orbitals. For most electroluminescent devices, poly (3,4-ethylenedioxthiophene): poly (4-styrenesulphonate) (PEDOT: PSS) is used as HIL while 2, 9-dimethyl-4,7- Diphenyl-1, 10-phenanthroline (BCP) is used as a hole blocking layer (HBL) [32]. The results obtained in our study show that only the HOMO energy values of compounds C_1 and C_2 are placed between those of (PEDOT: PSS) (-5.00 eV) and BCP (-6.50 eV) [33] (Figure 4). Determining the effectiveness of migration and injecting holes requires a difference in HOMO energy between the two types of compounds. It can be noted that the compound that has a HOMO energy close to that of PEDOT: PSS (-5.0 eV) is the compound C_2 (-5.156 eV), so this compound has a better migration capacity of the holes due to small energy barrier.

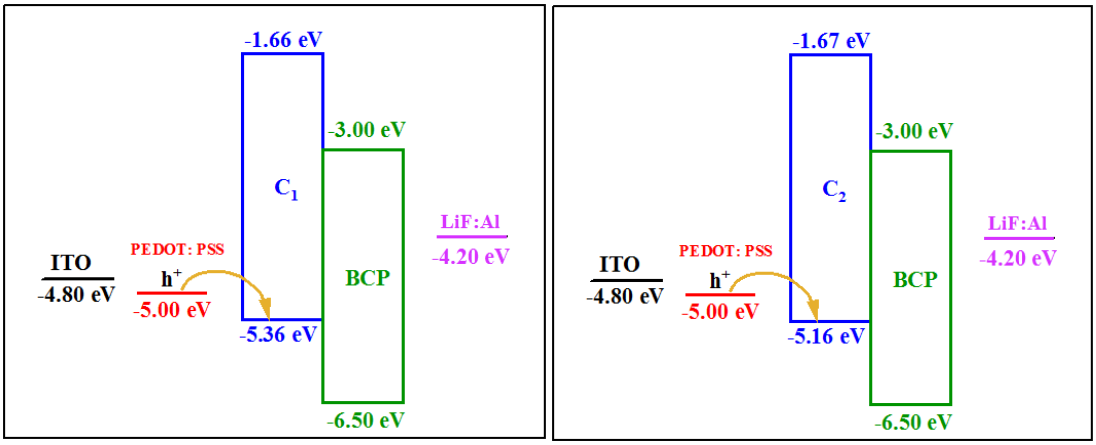

Figure 4: *Energy diagrams of compounds studied with the experimental values of PEDOT: PSS and BCP.*

3.3. Ionization potential and electronic affinities

Optimizing the performance and stability of OLED devices requires equilibred transport of electrons and injected holes. Indeed, many authors have reported that the redox stability of OLED devices is related to different physicochemical parameters such as ionization potential (IP) and electronic affinity (EA) [34, 35]. It should be noted that in order to have an easy injection of electrons (holes) into the emitting materials, they must have a high electron affinity and a low ionization potential. In this context, we have performed optimizations of studied structures C_1, C_2 and C_3, this time in the cationic and anionic states by using the same method of B3LYP/6-311G (d, p) and based on the geometries already optimized in the neutral state, we have calculated the values of the ionization potentials (IP) and those of the electronic affinities (EA) of the three compounds according to the following formulas:

$$\mathbf{IP} = \boldsymbol{E_0^+ - E^0} \quad \mathbf{(1)}$$

$$\mathbf{EA} = \boldsymbol{E^0 - E_0^-} \quad \mathbf{(2)}$$

$\boldsymbol{E^0}$: Energy in the neutral state.

($\boldsymbol{E_0^+}$,$\boldsymbol{E_0^-}$): Energies of the cationic and anionic states

Table 4: *IP, EA and reorganization energies for each molecule (in eV) calculated by the DFT / B3LYP / 6-311G (d, p).*

Compounds C_i	IP	EA	λ_{hole}	$\lambda_{electron}$	λ_{Total}
C_1	6.10	0.93	0.10	0.18	0.28
C_2	6.00	0.94	0.12	0.17	0.29
C_3	5.83	0.87	0.14	0.16	0.30

The results in Table 4 show that the obtained values of the ionization potential(IP) decrease in the following order: $C_1 > C_2 > C_3$ indicating the increase of the hole injection from the HTL layer to the HOMO level of the studied compound C_i. On the other hand, compound C_2 has the highest EA value (0.94 eV), indicating that it has a large electron-injecting capacity.

According to Marcus/Hush's model [35-37]. The transfer rate of the charge K (hole or electron) can be expressed by the following formula:

$$\boldsymbol{K = A.exp(-\frac{\lambda}{4K_B.T})} \quad \mathbf{(3)}$$

Where A is a factor which depends on the force of the electronic coupling between the emissive layer and the surface of the anode or cathode[33]. k_B is the Boltzmann constant. T is the temperature and λ is the reorganization energy due to the geometric relaxation accompanying the load transfer.

For OLED materials, load mobility has been shown to be mainly related to internal reorganization energyλ[38]. The reorganization energy λ for electron injection and hole transport can be expressed as follows [39-41]:

$$\boldsymbol{\lambda_{hole} = (E_0^+ - E_+^+) + (E_+^0 - E_0^0)} \mathbf{(4)}$$

$$\boldsymbol{\lambda_{electron} = (E_0^- - E_-^-) + (E_-^0 - E_0^0)} \mathbf{(5)}$$

Where $\boldsymbol{E_0^+}$($\boldsymbol{E_0^-}$) is the energy of cationic form (anionic form) calculated from the optimized structure of the neutral molecule. Similarly, $\boldsymbol{E_+^+}$ ($\boldsymbol{E_-^-}$) is the energy of cationic form (anionic form) calculated from

the optimized structure of the anionic state. $\boldsymbol{E_{+}^{0}}$ ($\boldsymbol{E_{-}^{0}}$) is the energy of the neutral molecule calculated at the cationic (anionic) state. Finally, $\boldsymbol{E_{0}^{0}}$ is the energy of the neutral molecule in its fundamental state. These two types of energy were calculated for all studied moleculesC_1, C_2 and C_3 and presented in Table 4. The obtained values indicate that the electron reorganization energies $\lambda_{electron}$ are slightly higher than those corresponding to the reorganization of the holes λ_{hole} for all compounds. These results clearly show that the compounds studied are better for the transport of holes than the injection of electrons.

3.4. *NBO analysis*

Natural-bonded orbital analysis (NBO) is an important tool for studying the binding and interaction between several molecules [42, 43]. NBO has a useful aspect to provide considerable information on inter- or intramolecular interactions in occupied and unoccupied orbital spaces in order to understand chemical phenomena such as hydrogen bonding and conjugal interactions in the molecular system [44– 46] .The delocalization of electronic density between filled and virtual orbital spaces (NBO) corresponds to a stabilizing donor-acceptor interaction [47-49]. To examine the donor-acceptor interaction involving the relocation of electrons from the occupied NBO to the unoccupied NBO, the second-order Fock matrix in the NBO database has been completed [42]. This donor-acceptor interaction can be expressed as secondary disturbance interaction energy E(2) [50]. In the NBO analysis, the highest energy E(2) indicates the strongest interaction between donors and electron acceptors that is a tendency for electron donors to contribute to electron acceptors which leads to a large combination of the entire system due to the delocalization of electrons [51, 52].

The hyper conjugative intramolecular interaction of the electrons σ and π of the C-C, C-H, C-N and N-H bonds with the anti-bonds C-C, C-H and C-N leads to the stabilization of part of the cycle. Natural-bound orbital analysis (NBO) has been performed based on the optimized structures at their fundamental states obtained with the DFT/B3LYP/6-311G (d, p) method. The results show that intermolecular interactions are created by the orbital overlap between the orbital C–C and C–C bonds anti-binders resulting in an intramolecular load transfer (ICT) involving stabilizing the system. The greatest intramolecular hyper conjugative interaction of electrons σ of (C_7–C_8), (C_{25}–C_{26}) and (C_{18}–C_{19})is distributed into σ* electrons of atoms (C_4–C_7), (C_{16}–C_{21}) and (C_{23}–C_{24}) of the rings of compounds C_1, C_2 and C_3 respectively.There are also a π/ π* interactions associated to the resonance, although the charge transfer from the bonding orbital π to antibonding orbital π* of the rings of molecules C_1, C_2 and C_3 respectively is predicted for the π C_{33}–C_{36}→ π* C_{31}–C_{32}, π C_{24}–C_{25}→ π* C_{26}–$C_{27}$and π C_{18}–C_{19}→ π* C_{18}–C_{19}.The intramolecular interaction π*- π*, n-π* and π-π* of molecules C_1, C_2 and C_3 respectively is formed by the orbital overlap between π* (C_{24} – C_{25}) - π* (C_{63} – C_{64}) with an energy of 100.8 Kcal/mol. As shown in Table 5, there are also interactions of σ-σ*, π-σ*, π*-σ*, n*-π*, n*-σ* and n-σ* that are less strong than interactions of π*-π*, n-π* and π-π*.

3.5. *Absorption and emission properties*

In order to predict the absorption properties of our studied conjugated compounds, time-dependent functional density TD–DFT / B3LYP / 6-311G (d. p) is used. With this method (TD-DFT), several absorption parameters have been calculated from previously optimized structures such as the electronic vertical transition energy (E_{Tr}), oscillator forces (f), maximum absorption wavelength (λ_{max}) and the nature of the transitions. So we have calculated these different parameters from the fully optimized structures of C_1, C_2 and C_3. The results are shown in Table 6 and the absorption spectra is shown in figure 5.

Table 5: *NBO Analysis*

molecule	type	DonorNBO (i)	Acceptor NBO(j)	E(2) kcal/mol	E(j)-(i) a.u	F (i.j) a.u
C_1	σ -σ*	10. BD (1) C_4–C_5	BD*(1) C_7–N_{11}	2.90	1.13	0.051
		16. BD (1) C_7–C_8	BD*(1) C_4–C_7	5.10	1.18	0.069
		101. BD (1) C_{64}–C_{65}	BD*(1) C_{63}–H_{75}	4 .78	1.06	0.064
		101. BD (1) C_{64}–C_{65}	BD*(1) N_{63}–H_{75}	5.24	1.04	0.066
		24. BD (1) C_{10}–N_{11}	BD*(1) C_7–N_{11}	1.99	1.25	0.045
		103. BD (1) C_{65}–N_{66}	BD*(1) C_{24}–C_{25}	3.65	1.33	0.063
		103. BD (1) C_{65}–N_{66}	BD*(1) C_{64}–H_{76}	3.01	1.26	0.055
		103. BD (1) C_{65}–N_{66}	BD*(1) N_{64}–H_{76}	0.92	1.21	0.030
		25. BD (1) C_{10}–H_{18}	BD*(1) C_7–N_{11}	3.51	1.00	0.053
		46. BD (1) C_{26}–H_{37}	BD*(1) C_{25}–H_{40}	0.82	0.87	0.025
		53. BD (1) C_{29}–H_{40}	BD*(1) C_{25}–C_{26}	4.69	1.04	0.063
		53. BD (1) N_{11}–H_{19}	BD*(1) C_7–C_8	1.8	1.27	0.043
	π*-σ*	912. BD (2) C_3–C_4	BD*(1) C_7–N_{11}	0.55	0.42	0.030
	π*- π*	943. BD* (2) C_{24}–C_{25}	BD*(2) C_{63}–C_{64}	100.8	0.02	0.068
	π - π*	61. BD (2) C_{33}–C_{36}	BD*(2) C_{31}–C_{32}	23.82	0.27	0.071
	π - σ*	2. BD (2) C_1–C_2	BD*(1) C_{20}–C_{62}	1.09	0.81	0.029
		8. BD (2) C_3–C_4	BD*(1) C_7–N_{11}	0.78	0.70	0.023
		70. BD (2) C_{45}–C_{46}	BD*(1) C_{47}–H_{74}	2.14	0.68	0.037
	n - π*	152. LP (1) C_{30}	BD*(2) C_{26} - C_{29}	54.45	0.14	0.101
	n*- π*	153. LP*(1) C_{46}	BD*(2) C_{45} - C_{46}	32.7	0.12	0.067
	n*-σ*	153. LP*(1) C_{46}	BD*(1) C_{46} - C_{47}	7.35	0.72	0.094
	n -σ*	154. LP (1) C_{65}	BD*(1) C_{24} - N_{66}	10.39	0.67	0.076
		154. LP (1) C_{65}	BD*(1) C_{63} - C_{64}	4.18	0.85	0.055
		154. LP (1) C65	BD*(1) N66 - H67	1.60	0.67	0.030
C_2	σ -σ*	15. BD (1) C_6–C_8	BD*(1) C_4–N_5	3.72	1.04	0.056
		58. BD (1) C_{25}–C_{26}	BD*(1) C_{23}–C_{24}	6.82	1.10	0.077
		1. BD (1) C_1–C_2	BD*(1) C_3–H_{49}	4.74	1.10	0.065
		5. BD (1) C_2–C_4	BD*(1) N_5–H_{50}	2.94	1.16	0.052
		8. BD (1) C_3–N_5	BD*(1) C_4–N_5	1.13	1.17	0.033
		8. BD (1) C_3–N_5	BD*(1) C_4–C_5	4.01	1.25	0.064
		8. BD (1) C_3–N_5	BD*(1) C_1–H_{47}	3.27	1.28	0.058
		10. BD (1) C_4–N_5	BD*(1) N_5–H_{50}	1.91	1.41	0.046
		7. BD (1) C_{20}–H_{48}	BD*(1) C_4–N_5	3.56	0.94	0.052
		20. BD (1) C_8–H_{52}	BD*(1) C_9–H_{83}	0.85	1.03	0.026
		20. BD (1) C_8–H_{52}	BD*(1) C_9–C_{11}	5.22	1.01	0.065
		12. BD (1) N_5–H_{50}	BD*(1) C_2–C_4	1.41	1.32	0.039
	π - π*	56. BD (2) C_{24}–C_{25}	BD*(2) C_{26}–C_{27}	14.36	0.31	0.062
		14. BD (2) C_6–C_7	BD*(2) C_4–N_5	0.59	0.67	0.019
	π - σ*	24. BD (2) C_{10}–C_{11}	BD*(1) C_{12}–C_{15}	2.08	0.74	0.037
		56. BD (2) C_{24}–C_{25}	BD*(1) N_{42}–H_{74}	0.78	0.70	0.022
		67. BD (2) C_{28}–C_{30}	BD*(1) C_{27}–N_{42}	0.85	0.67	0.023
	n - π*	154. LP (1) N_5	BD*(2) C_2– C_4	28.95	***	***
C_3	σ -σ*	65. BD (1) C_{28}–C_{29}	BD*(1) C_{27}–N_{46}	3.95	1.05	0.057
		43. BD (1) C_{18}–C_{19}	BD*(1) C_{16}–C_{21}	6.76	1.12	0.078
		8. BD (1) C_3–C_{23}	BD*(1) C_{22}–H_{60}	3.26	1.11	0.054
		40. BD (1) C_{17}–C_{18}	BD*(1) N_{24}–H_{62}	0.52	1.12	0.022
		49. BD (1) C_{20}–N_{24}	BD*(1) C_{21}–N_{46}	2.41	1.17	0.047
		42. BD (1) C_{17}–N_{24}	BD*(1) C_{20}–C_{21}	4.51	1.26	0.068
		42. BD (1) C_{17}–N_{24}	BD*(1) C_{18}–H_{58}	3.08	1.23	0.055
		49. BD (1) C_{20}–N_{24}	BD*(1) N_{24}–H_{62}	0.84	1.17	0.028
		44. BD (1) C_{18}–H_{58}	BD*(1) C_{17}–N_{24}	3.73	0.94	0.053
		4. BD (1) C_1–H_{47}	BD*(1) C_3–H_{49}	0.82	0.99	0.026
		72. BD (1) C_{30}–H_{66}	BD*(1) C_{28}–C_{29}	5.93	1.00	0.069
		57. BD (1) N_{24}–H_{62}	BD*(1) C_{17}–C_{18}	4.54	0.66	0.052
	π - π*	67. BD (2) C_{28}–C_{30}	BD*(2) C_{26}–C_{27}	16.36	0.31	0.064

	π - σ*	**41. BD (2) C_{17}–C_{18}**	**BD*(1) N_{24}–H_{62}**	**3.28**	**0.67**	**0.044**
	n - π*	**154. LP (1) N_{24}**	**BD*(2) C_{17}– C_{18}**	**11.67**	**0.38**	**0.061**
	n -σ*	**154. LP (1) N_{24}**	**BD*(1) C_{19}– C_{20}**	**2.38**	**0.97**	**0.045**
		154. LP (1) N_{24}	**BD*(1) N_{24}–H_{62}**	**1.46**	**0.75**	**0.031**

Table 6: *Absorption parameters data of the studied compounds obtained by TD-DFT/B3LYP/ 6-311G (d. p).*

Compounds	λ_{abs} (nm)	E_{tr} (eV)	O.S	MO/Character
C_1	413.305	2.999	2.944	HOMO->LUMO (96%)
C_2	428.874	2.891	2.566	HOMO->LUMO (97%)
C_3	443.796	2.793	2.408	HOMO->LUMO (98%)

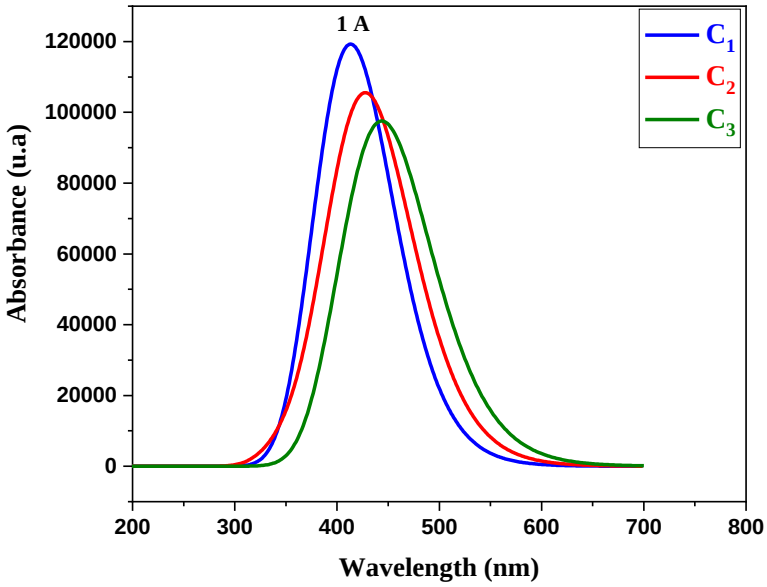

Figure 5: UV-vis absorptionspectra of the studied molecules obtained by TD-DFT/ B3LYP/6-311G (d. p).

The results of Table 6 show intense absorption bands in the range of 297 to 715 nm, these high absorption bands for each molecule generally correspond to an excitation of the electrons of the HOMO → LUMO level and an electronic transition of type π–π*. However, the molecules C_1, C_2 and C_3 show their highest absorption respectively at 413.305 nm, 428.874 nm and 443.796 nm. In addition, we have observed shoulders in the absorption spectra of the studied molecules, which results in intramolecular charge transfers [29]. As a result, these organic compounds can capture light in a wide wavelength range.

On the other hand and in order to study the emission properties of the studied compounds C_1, C_2 and C_3, the TD/B3LYP/6–311G (d. p) method has been used on the basis of optimized geometries [53]. Quantum chemical calculations of the emission properties of these compounds are presented in Table 7.

Table 7: *Emission parameters data obtained by the TD-DFT-B3LYP/6-311G (d. p) method for the compounds studied.*

Compounds	E (eV)	λ_{em}(nm)	Stocks Shift (SS) (nm)
C_1	2.637	470.115	56.81
C_2	2.546	486.954	58.08
C_3	2.470	501.956	58.16

The results show that emission spectra are attributed to LUMO → HOMO electron transitions for all molecules. It is noted that theoretical photoluminescence spectra of the studied molecules have a maximum at 470.115nm, 486.954 nm and 501.956 nm for C_1, C_2 and C_3 respectively (Table 7 and figure 6). The stoke shift is related to the wavelengths of the absorption and emission bands[54, 55] and is determined by calculating the difference between the absorption and emission maximums. Stocks Shift (SS) values are relatively low for all studied compounds:C_1 (56.81nm), C_2 (58.08 nm) and C_3 compounds (58.16 nm). As a result, molecules with a low Stokes Shift show a minimal conformational reorganization between the fundamental and excited states.

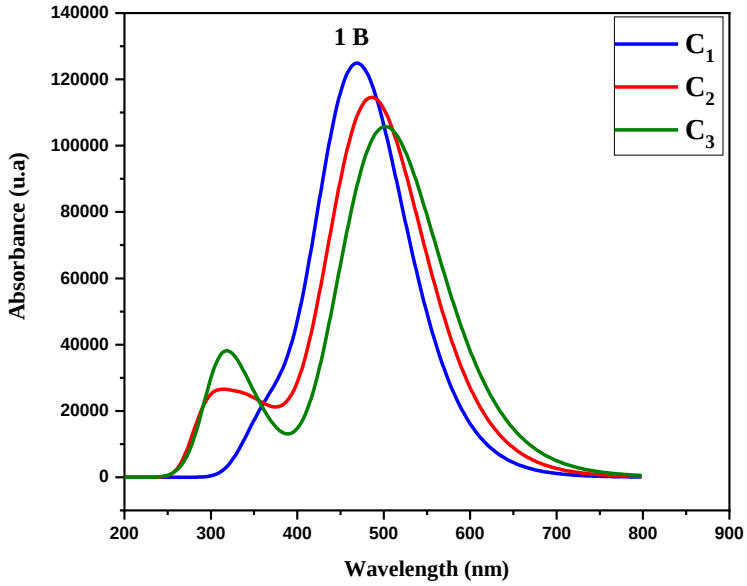

Figure 6: Emission spectra of the studied molecules obtained by TD-DFT/ B3LYP/6-311G (d. p).

Conclusion

In this work, a quantum chemical study was carried out on organic compounds based on terphenyl and pyrrole. All molecules exhibit more or less distorted structures due to the electronic nature of the aryl and pyrrole nuclei. The DFT quantum method and its TD-DFT approaches have been used for the study of geometric structures, optoelectronic properties, intramolecular charge transfer (ICT), load mobility performance, absorption and emission properties. The results reveal that the studied compounds generally have prohibited band energies which make them good candidates for applications as multifunctional and bifunctional OLED materials. This is demonstrated by the calculation of ionization potentials (IP) and electronic affinities (EA). The energies of reorganization of electrons λelectron are slightly large as their energies of reorganization of holes λ_{hole} for all compounds; this means that these compounds are better for carrying holes than electron injection and therefore can act as emitters in OLEDs. The calculated UV-vis absorption spectra of all compounds present at an electron excitation of the HOMO → LUMO level and an electronic transition of the type π–π* (phosphorus transition character) at approximately 400 nm.

In summary, the studied structures have a large prohibited band (greater than 3 eV) due to intermolecular load transfer. The calculated IP values decrease slightly indicating the increase in hole injection facilities from the HTL layer to the HOMO level. Therefore, the studied compounds C_1, C_2 and C_3 have improved electroluminescent properties.

References

1. Y. Karzazi,Organic light emitting diodes: Devices and applications, *J. Mater. Environ. Sci.*, 5(1) (2014) 1–12.
2. H. Derouiche and V. Djara,Impact of the energy difference in LUMO and HOMO of the bulk heterojunctions components on the efficiency of organic solar cells, *Sol. Energy Mater. Sol. Cells*, 91 (13) (2007) 1163–1167. DOI:10.1016/j.solmat.2007.03.015
3. M. Bourass,A.T.Benjelloun, M. Benzakour, M.Mcharfi, F.Jhilal, F.S, Spirau,J.M. Sotiropoulos, M. Bouachrine, DFT/TD-DFT characterization of conjugational electronic structures and spectral properties of materials based on thieno[3,2-b][1]benzothiophene for organic photovoltaic and solar cell applications, *J. Saudi Chem. Soc*, 21(5) (2019) 563–574. DOI:10.1016/j.jscs.2017.01.001
4. M. R. Azrain,M.R. Mansor, G. Omar, S.H.S.M. Fadzullah, S.R. Esa, L.M. Lim, D. Sivakumar, M.N.A. Nordin, Effect of high thermal stress on the organic light emitting diodes (OLEDs) performances, *Synth. Met.* 247 (2018) 191–201. DOI:10.1016/j.synthmet.2018.12.008
5. H. Chen, Q. Cui, G.Yu, Y. Guo, J. Huang,M. Zhu, X. Guo, Y. Liu, Synthesis and characterization of novel semiconductors based on thieno[3,2- b][1]benzothiophene Cores and their applications in the organic thin-film transistors, *J. Phys. Chem. C*, 115 (48) (2011) 23984–23991. DOI:10.1021/jp2081484
6. H. Ebata, E. Miyazaki, T. Yamamoto, K. Takimiya, Synthesis, properties, and structures of benzo[1,2-b:4,5-b′]bis[b] benzothiophene and benzo[1,2-b:4,5-b′]bis[b]benzoselenophene, *Org. Lett*. 9(22) (2007) 4499–4502. DOI:10.1021/ol701815j
7. O. Taby, C.L. Rosenfield, V. Bogdanov, Y. Nemerson, M. B. Taubman, Cloning of the rat tissue factor cDNA and promoter: Identification of a serum-response region, *Thromb. Haemost*. 76(5) (1996) 697–702.
8. M. C. Hamilton, S. Martin, J. Kanicki, Thin-film organic polymer phototransistors. IEEE Trans Electron Devices, *IEEE Trans. Electron Devices*. vol. 51(6) (2004) 877–885. DOI:10.1109/TED.2004.829619
9. Li Gang, V. Shrotriya, J. Huang, Y. Yao, T. Moriarty, K. Emery, Y. Yang, Self-Organization of Polymer Blends, *Nature Materials*, 4 (2005) 864-868. DOI: 10.1038/nmat1500
10. P. Peumans, A. Yakimov, S. R. Forrestn, Small molecular weight organic thin-film photodetectors and solar cells, *J. Appl. Phys*, 93 (2003) 3693–3723.DOI: 10.1063/1.1534621
11. B. Lüssem, M. Furno, K. Leo, Highly efficient pin-type OLEDs, *Org. Light. Diodes*, (2013) 173–191 DOI:10.1533/9780857098948.2.173
12. C. W. Tang, S. A. Vanslyke, Organic electroluminescent diodes. *Appl. Phys. Lett*. 51(12) (1987)913–915. DOI:10.1063/1.98799
13. A. Lääperi, Active Matrix, Organic Light-Emitting Diodes (AMOLEDs)for Displays, *Woodhead Publishing Limited*,(2013).DOI:10.1533/9780857098948.3.445
14. C. Adachi, T. Tsutsui, S. Saito,Blue light-emitting organic electroluminescent devices, *Appl. Phys. Lett*, 56(9)(1990)799–801. DOI: 10.1063/1.103177
15. J. Salbeck, Electroluminescence with Organic Compounds, *Ber. Bunsenges. Phys. Chem*, 100(10) (1996) 1667–1677. DOI:10.1002/bbpc.19961001002
16. J. Roncali,Molecular engineering of the band gap of π-conjugated systems: Facing technological applications, *Macromol. Rapid Commun*, 28(17) (2007)1761–1775. DOI:10.1002/marc.200700345
17. H. B. Dias, K. N. Bourdakos,V. Jankus, K. C. Moss, K. T. Kamtekar, V. Bhalla, J. Santos, M. R. Bryce, A.P. Monkman, Triplet harvesting with 100% efficiency by way of thermally activated delayed fluorescence in charge transfer OLED emitters, *Adv. Mater*. 25(27) (2013)3707–3714. DOI:

10.1002/adma.201300753
18. H. Wang, L. Xie, Q. Peng,L. Meng, Y. Wang, Y. Yi, P. Wang, Novel thermally activated delayed fluorescence materials-thioxanthone derivatives and their applications for highly efficient OLEDs, *Adv. Mater*. 26(30)(2014) 5198–5204. DOI:10.1002/adma.201401393
19. Yi. Im and J. Y. Lee,Above 20% external quantum efficiency in thermally activated delayed fluorescence device using furodipyridine-type host materials, *Chem. Mater*, 26(3) (2014) 1413–1419. DOI:10.1021/cm403358h
20. S. Bouzakraoui, S.M. Bouzzine,M. Bouachrine, M. Hamidi, Theoretical investigation of electroluminescent alkoxy substituted 4,4′-bis(2-phenylethenyl)biphenyls as guest in blue OLEDs, *Sol. Energy Mater. Sol. Cells*. 90(10) (2006) 1393–1402. DOI: 10.1016/j.solmat.2005.10.004
21. M. Witwicki and J. Jezierska,Protic and aprotic solvent effect on molecular properties and g-tensors of o-semiquinones with various aromacity and heteroatoms: A DFT study, *Chem. Phys. Lett*. 493(4–6) (2010)364–370. DOI: 10.1016/j.cplett.2010.05.063
22. A. D. Becke, A new mixing of Hartree-Fock and local density-functional theories, *J. Chem. Phys*. 98(2)(1993)1372–1377. DOI:10.1063/1.464304
23. C. Lee, W. Yang, R. G. Parr,Development of the Colle-Salvetti correlation-energy formula into a functional of the electron density, *Phys. Rev. B*. 37 (2)(1988) 785-789. DOI:10.1103/PhysRevB.37.785
24. G. E. Frisch, M. J. Trucks, G. W. Schlegel, H. B, Scuseria, B. Robb, M. A. Cheeseman, J. R. Scalmani, G. Barone, V. Mennucci et al. "Gaussian 09." Wallingford. p. Revision A.02. 2009.
25. S. Boussaidi, H. Zgou, A. Eddiouane, H. Chaib,New π -conjugated oligomers containing thiophene and phenylene rings with low band-gap for solar cell applications : a DFT study, *J. Comput. Methods Mol. Des.* 5(3) (2015) 1–9.
26. J. Roncali,Synthetic Principles for Bandgap Control in Linear pi-Conjugated Systems, *Chem. Rev*. 97 (1997) 173–205. DOI: 10.1021/cr950257t
27. M.Bourass, A.T Benjelloun, M.Benzakour,M. Mcharfi,M. Hamidi,S.M. Bouzzine, M. Bouachrine, DFT and TD-DFT calculation of new thienopyrazine-based small molecules for organic solar cells, *Chem. Cent. J*, 10(1) (2016) 1–11. DOI:10.1186/s13065-016-0216-6
28. H. Zgou. S. Boussaidi A. Zahlou. M. Bouachrine and M. Hamid Donor-Acceptor Organic Materials with low Band-gap for Photovoltaic Applications : a Theoretical Investigation. *Int. J. Adv. Res. Comput. Sci. Softw. Eng.*4(5)(2014)10–19.
29. L. Yang, J.K. Feng,A.M. Ren,Theoretical studies on the electronic and optical properties of two thiophene-fluorene based π-conjugated copolymers, *Polymer*. 46(24) (2005) 10970–10981. DOI:10.1016/j.polymer.2005.09.050
30. R. E. Stratmann, G. E. Scuseria, M. J. Frisch, An efficient implementation of time-dependent density-functional theory for the calculation of excitation energies of large molecules, *J. Chem. Phys.*109(19)(1998) 8218–8224. DOI:10.1063/1.477483
31. M. Saoudi, R.Ajjel and B. Zaidi,Experimental and theoretical study on the charge transfer between polyaniline and single walled carbon nanotubes, *J. Mater. Environ. Sci. 7 (12) (2016) 4435-4447*
32. A. M. Thangthong, D. Meunmart, N. Prachumrak, S. Jungsuttiwong, T. Keawin, T. Sudyoadsuk, V. Promarak, Synthesis and characterization of 9,10-substituted anthracene derivatives as blue light-emitting and hole-transporting materials for electroluminescent devices, *Tetrahedron*. 68(7) (2012) 1853–1861. DOI:10.1016/j.tet.2011.12.083
33. M. Bourass, N. Komiha, O. K. Kabbaj, N. Wazzan, M. Chemek, M. Bouachrine, The photophysical properties and electronic structures of bis[1]benzothieno[6,7- d :6′,7′- d ′]benzo[1,2- b :4,5- b

′]dithiophene (BBTBDT) derivatives as hole-transporting materials for organic light-emitting diodes (OLEDs), *New J. Chem*. 43(40) (2019) 15899-15909. DOI:10.1039/C9NJ02756D
34. L. Y. Zou, A. M. Ren, J. K. Feng, X. Q. Ran,Theoretical design study on multifunctional triphenyl amino-based derivatives for OLEDs, *J. Phys. Org. Chem.* 22(11) (2009) 1104–1113. DOI 10.1002/poc.1565
35. E. Louis, E. San-Fabián, M. A. Díaz-García, G. Chiappe, J. A. Vergés,Are Electron Affinity and Ionization Potential Intrinsic Parameters to Predict the Electron or Hole Acceptor Character of Amorphous Molecular Materials. *J. Phys. Chem. Lett.* 8(11) (2017) 2445–2449. DOI:10.1021/acs.jpclett.7b00681
36. N. S. Hush, Adiabatic rate processes at electrodes. I. Energy-charge relationships, *J. Chem. Physn.* 28(5)(1958)962–972. DOI:10.1063/1.1744305
37. R. A. Marcus, Electron Transfer Reactions in Chemistry: Theory and Experiment, *Noyes Laboratory of Chemical Physics*. 32(8)(1993) 1111–1121.DOI:10.1002/anie.199311113
38. R. A. Marcus, On the theory of oxidation-reduction reactions involving electron transfer, *J. Chem. Phys.* 24(5) (1956) 966–978. DOI:10.1063/1.1742723
39. M. Malagoli and J. L. Brédas,Density functional theory study of the geometric structure and energetics of triphenylamine-based hole-transporting molecules, *Chem. Phys. Lett.* 327(1–2) (2000) 13–17. DOI:10.1016/S0009-2614(00)00757-0
40. Y. Z. Lee, X. Chen, S. A. Chen, P. K. Wei, W. S. Fann,oluble electroluminescent poly(phenylene vinylene)s with balanced electron- and hole injections, *J. Am. Chem. Soc.*123(10) (2001) 2296–2307. DOI:10.1021/ja003135d
41. R. F. Jin and Y. F. Chang, A theoretical study on photophysical properties of triphenylamine-cored molecules with naphthalimide arms and different π-conjugated bridges as organic solar cell materials" *Phys. Chem. Chem. Phys*, 17(3)(2015)2094–2103.DOI:10.1039/C4CP04394D
42. G. R. Hutchison, M. A. Ratner, T. J. Marks,Hopping transport in conductive heterocyclic oligomers: Reorganization energies and substituent effects, *J. Am. Chem. Soc*, 127(7) (2005) 2339–2350. DOI:10.1021/ja0461421
43. E. Gladis Anitha, S. Joseph Vedhagiri, K. Parimala, Conformational stability, vibrational spectra, NLO properties, NBO and thermodynamic analysis of 2-amino-5-bromo-6-methyl-4-pyrimidinol for dye sensitized solar cells by DFT methods, *Spectrochim. Acta - Part A Mol. Biomol. Spectrosc.* 140 (2015) 544–562. DOI:10.1016/j.saa.2014.12.017
44. F. Weinhold, C. R. Landis, E. D. Glendening, What is NBO analysis and how is it useful.*Int. Rev. Phys. Chem*, 35(3) (2016) 399–440.DOI:10.1080/0144235X.2016.1192262
45. S. Murugavel, P. S. Kannan, A. Subbiahpandi, T. Surendiran, S. Balasubramanian, 2,3,4,9-Tetra-hydro-1H-carbazole, *Acta Crystallogr. Sect. E*, 64(12)(2008)0–6. DOI:10.1107/S1600536808038713
46. G. Shakila, H. Saleem, N. Sundaraganesan,FT-IR, FT-Raman, NMR and U-V Spectral investigation : Computation of vibrational frequency , chemical shifts and electronic structure calculations of 1-bromo-4-nitrobenzenen. *World Scientific News.* 61(2) (2017)150–185.
47. C. M. Rohlfing, L. C.Allen, R. Ditchfield,Proton and carbon-13 chemical shifts: Comparison between theory and experiment, *Chem. Phys. 87*(1)(1983)9–15. DOI:10.1016/0301-0104(84)85133-2
48. A. E. Reed, L. A. Curtiss, F. Weinhold,Intermolecular Interactions from a Natural Bond Orbital, Donor—Acceptor Viewpoint, *Chem. Rev.* 88(6)(1988) 899–926. DOI:10.1021/cr00088a005
49. J. E. Carpenter and F. Weinhold,Analysis of the geometry of the hydroxymethyl radical by the "different hybrids for different spins" natural bond orbital procedure, *J. Mol. Struct. THEOCHEM*. 169(1988) 41–62. DOI:10.1016/0166-1280(88)80248-3

50. J. N. Liu, Z. R. Chen, S. F. Yuan,Study on the prediction of visible absorption maxima of azobenzene compounds, *J. Zhejiang Univ. Sci B*, 6(6)(2005)584–589.DOI: 10.1631/jzus.2005.B0584
51. A. Zülfikaroğlu, H. Batı, N. Dege,A theoretical and experimental study on isonitrosoacetophenone nicotinoyl hydrazone: Crystal structure, spectroscopic properties, NBO, NPA and NLMO analyses and the investigation of interaction with some transition metals, *J. Mol. Struct.* 1162(2018)125–139.DOI:10.1016/j.molstruc.2018.02.079
52. M. Bourass, A. T. Benjelloun, M. Benzakour,M. Mcharfi, F. Jhilal, F. S. Spirau, J. M. Sotiropoulos, M. Bouachrine, DFT/TD-DFT characterization of conjugational electronic structures and spectral properties of materials based on thieno[3,2-b][1]benzothiophene for organic photovoltaic and solar cell applications, *J. Saudi Chem. Soc*. 21(5)(2017) 563–574.DOI:10.1016/j.jscs.2017.01.001
53. M. Bourass, A. T. Benjelloun, M. Benzakour, M. Mcharfi, F. Jhilal, M. Hamidi, M.Bouachrine,The optoelectronic properties of organic materials based on triphenylamine that are relevant to organic solar photovoltaic cells, *New J. Chem.* 41(22)(2017)13336–13346.DOI:10.1039/C7NJ03272B
54. M. Bourass, A. T. Benjelloun, M. Benzakour, M. Mcharfi, M. Hamidi, S.M. Bouzzine, F. S. Spirau, T. Jarrosson, J. P. Lère-Porte, J. M. Sotiropoulos, M. Bouachrine,The computational study of the electronic and optoelectronics properties of new materials based on thienopyrazine for application in dye solar cells, *J. M. E. S.* 7(3) (2016) 700–712.
55. Young-Kyu Han,Time-dependent density functional study of electroluminescent polymers, *J. Phys. Chem. A.* 108(42)(2004) 9316–9318. DOI:10.1021/jp037746e
56. A. Azazi, A. Mabrouk, K. Alimi,Theoretical investigation on the photophysical properties of low-band-gap copolymers for photovoltaic devices, *Comput. Theor. Chem.* 978(1–3) (2011) 7-15. DOI:10.1016/j.comptc.2011.08.020

(2020) ; http://www.jmaterenvironsci.com